Mechanisms Regulating the Cell Surface Residence Time of the α_{2A}-Adrenergic Receptor†

Matthew H. Wilson and Lee E. Limbird*

Department of Pharmacology, Vanderbilt University Medical Center, Nashville, Tennessee 37232-6600

Received August 30, 1999; Revised Manuscript Received November 2, 1999

ABSTRACT: Despite considerable insights concerning the mechanisms regulating short-term agonist-mediated G protein-coupled receptor (GPCR) internalization, little is known about the mechanisms regulating GPCR surface residence over long periods of time. Herein, we experimentally evaluated mechanisms regulating the surface $t_{1/2}$ of various α_{2A}-adrenergic receptor (α_{2A}AR) structures. The Δ3iα_{2A}AR (lacking the third intracellular loop), D79Nα_{2A}AR (impaired G protein coupling), and CAMα_{2A}AR (enhanced G protein coupling) all exhibited a cell surface α_{2A}AR turnover in Chinese hamster ovary cells that was faster than that of the wild type (WT). Cell surface receptor turnover could be slowed with ligand occupancy of D79Nα_{2A}AR (agonist or antagonist) and CAMα_{2A}AR (antagonist only) but not the Δ3i- or WTα_{2A}AR. This selective ligand-induced surface stabilization was paralleled by a dramatic ligand-dependent receptor density upregulation for D79N- and CAMα_{2A}AR structures. Receptors which exhibited surface turnover and density that could be modulated by ligand (D79N and CAM) also demonstrated structural instability, measured by a loss of radioligand binding capacity in detergent solution over time without parallel changes in receptor protein content. In contrast, the shorter surface $t_{1/2}$ of the Δ3iα_{2A}AR, whose cell surface $t_{1/2}$ and steady state density were not altered by ligand occupancy, occurred in the context of a structurally stable receptor in detergent solution. These results demonstrate that changes in receptor structure which alter receptor−G protein coupling (either an increase or decrease) are paralleled by structural instability and ligand-induced surface stabilization. These studies also provide criteria for assessing the structural instability of the α_{2A}AR that can likely be generalized to all GPCRs.

The α_2-adrenergic receptors (α_2ARs)[1] belong to a superfamily of seven transmembrane domain-containing G protein-coupled receptors (GPCRs) and couple through Gi/Go proteins to regulate multiple physiological processes (*1*). GPCRs serve to transduce signals from the extracellular to the intracellular environment. Consequently, the residence time of a receptor population on the cell surface is important in regulating GPCR function. Although much research has focused on the mechanisms of agonist regulating short-term surface residence time of GPCR (minutes) (*2*), little is known about possible mechanisms regulating GPCR cell surface residence over long periods of time (hours).

The α_{2A}AR serves as an excellent candidate for evaluation of the mechanisms regulating the long-term cell surface residence time of a GPCR. The α_{2A}AR has been shown to be localized at the surface when expressed in cells (*3*−*5*) and does not appear to undergo significant short-term agonist-mediated receptor internalization (*3*−*7*). Additionally, mutagenesis has revealed that the predicted third intracellular loop of the receptor appears to be important in regulating the surface $t_{1/2}$ of the α_{2A}AR on the basolateral surface of Madin Darby Canine Kidney II (MDCK II) cells, while other mutations affecting receptor glycosylation, palmitoylation, or deletion of the carboxy-terminal tail of the α_{2A}AR do not alter α_{2A}AR surface $t_{1/2}$ (*8*). More recent studies have suggested that the bulk of the third intracellular loop may be sufficient to stabilize the α_{2A}AR on the basolateral surface of MDCK II cells (*9*).

The studies presented here demonstrate that transient expression in Chinese hamster ovary (CHO) cells reveals surface turnover results indistinguishable from those achieved for the wild type and Δ3iα_{2A}AR on the basolateral surface of polarized MDCK II cells. Consequently, this transient expression system was used to evaluate the surface $t_{1/2}$ of other mutant α_{2A}AR structures to gain a further understanding of the mechanisms regulating the surface $t_{1/2}$ of GPCRs. We found that α_{2A}ARs with either impaired [D79N (*10*−*14*) (Figure 1)] or enhanced [constitutively active mutant (CAM) (*15*) (Figure 1)] coupling to G proteins exhibited a shorter

† This work was supported by National Institutes of Health Grants HL43671 and HL25182 to L.E.L. M.H.W. was supported in part by National Institutes of Health Medical Scientist Training Program Grant GM07347.

* To whom correspondence should be addressed: Department of Pharmacology, Vanderbilt University Medical Center, 468 MRB I, Nashville, TN 37232-6600. Phone: (615) 343-3538. Fax: (615) 343-6532. E-mail: lee.limbird@mcmail.vanderbilt.edu.

[1] Abbreviations: α_2AR, α_2-adrenergic receptor; GPCR, G protein-coupled receptor(s); WT, wild type; CHO, Chinese hamster ovary; CAM, constitutively active mutant; HA, hemagglutinin; FCS, fetal calf serum; COSM6, simian kidney fibroblasts; HEK293, human embryonic kidney cells; DMEM, Dulbecco Modified Eagle's Medium; DβM/CHS, dodecyl β-D-maltoside/cholesteryl hemisuccinate; PAGE, polyacrylamide gel electrophoresis; PBS, phosphate-buffered saline; $t_{1/2}$, half-life; Δ3iα_{2A}AR, Δaa240−359α_{2A}-adrenergic receptor (lacks the predicted third intracellular loop but retains regions required for G protein coupling); [^{125}I]PIC, [^{125}I]-*p*-iodoclonidine; TM, transmembrane domain.

10.1021/bi9920275 CCC: $19.00
Published on Web 01/04/2000

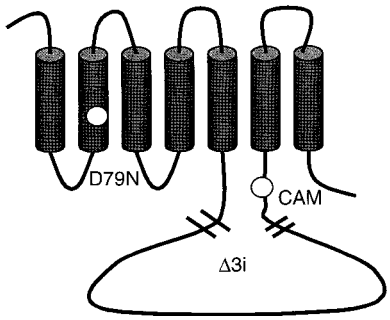

FIGURE 1: Schematic model of the α_{2A}AR depicting mutations which alter cell surface receptor residence time. The D79N mutation refers to the mutation of the highly conserved asparate located in TM2 (*40*). The CAM mutation refers to the T373K mutation at the base of TM6 resulting in constitutive activity (*15*). The Δ3i mutation refers to the deletion of amino acides 240−359 [lacking the predicted third intracellular loop but retaining regions required for G protein coupling (*8*, *9*)].

surface $t_{1/2}$ when compared to that of wild type α_{2A}AR, but that this accelerated surface turnover was delayed by ligand occupancy resulting in a ligand-induced increase in steady state receptor density. These effects of ligand suggest that the D79N- and CAMα_{2A}AR are structurally unstable, corroborated by the accelerated loss of functional binding capacity in detergent solution without the loss of protein content. In contrast, the Δ3iα_{2A}AR, which demonstrates an accelerated surface turnover when compared to that of WTα_{2A}AR, is not structurally unstable on the basis of findings of structural stability in detergent solution and the lack of an effect of ligand occupancy on either surface $t_{1/2}$ or steady state receptor density. These results suggest that structural instability, imparted by receptor mutations that alter receptor−G protein coupling, can result in cell surface receptor turnover that can be modulated by occupancy of receptor with ligand, revealing previously unappreciated mechanisms regulating cell surface residence of GPCRs over long periods of time. However, as is shown for the Δ3iα_{2A}-AR, enhanced surface turnover is not necessarily indicative of a structurally unstable receptor. Loss of functional binding capacity in detergent (in the absence of parallel loss of protein) and ligand-stabilized surface stability paralleled by ligand-dependent receptor density upregulation are more diagnostic indicators of structural instability.

EXPERIMENTAL PROCEDURES

Materials. Nitrocellulose membranes were purchased from Pharmacia. [^{3}H]Yohimbine was purchased from Dupont-NEN and [^{3}H]RX821002 from Amersham. HA.11 antibody was purchased from BABCo. Dodecyl β-D-maltoside and cholesteryl hemisuccinate were purchased from Calbiochem. Sulfo-NHS-biotin was purchased from Pierce. Epinephrine was obtained from Sigma and ascorbic acid from Fisher. Idazoxan was obtained from Research Biochemicals International. EcR-CHO cells were obtained from Invitrogen. Hemagglutinin (HA)-tagged α_{2A}AR, D79Nα_{2A}AR, and Δ3iα_{2A}AR have been described previously (*8*, *10*). The CAMα_{2A}AR (T373K mutation) was a generous gift from R. J. Lefkowitz (*15*).

Cell Culture and Transfection. EcR-CHO (Chinese hamster ovary cells engineered for the ecdysone-inducible expression system obtained from Invitrogen) cells were maintained in Ham's F12 medium supplemented with 10% fetal calf serum (FCS), 2 mM glutamine, and 100 units/mL penicillin G sodium with 100 μg/mL streptomycin sulfate (pen-strep). Simian kidney fibroblast (COS M6) cells were maintained in Dulbecco Modified Eagle's Medium (DMEM) supplemented with 10% FCS, 20 mM HEPES, and pen-strep. Cells were plated the day before transfection at a density of 2×10^6 (EcR-CHO) or 2.5×10^6 (COS) cells per well of a six-well plate. Cells were transiently transfected with the use of FuGENE-6 (Boehringer Mannheim) according to the manufacturer's instructions. Cells were assayed approximately 48 h post-transfection. Stably transfected EcR-CHO cells were obtained by a calcium phosphate precipitation method by cotransfecting a pCMV4 plasmid containing the receptor cDNA along with a plasmid harboring neomycin resistance (*8*). Stably transfected cells were selected through growth in 500 μg/mL G418 and assayed for receptor expression with radioligand binding analysis.

Binding in Cultured Cells. Treatment of cells began 24 h post-transfection. EcR-CHO cells were incubated with serum free medium containing 0.1 mM ascorbate alone or ascorbate with 100 μM epinephrine or 10 μM idazoxan. After treatment (for 16−24 h), cells were washed three times with phosphate-buffered saline (PBS) (pH 7.4) prewarmed to 37 °C. Triplicate wells of a six-well plate for transient transfectants or one 60 mm dish for stable transfectants was then scraped and the residue pooled in 1.2 mL of ice-cold buffer consisting of 25 mM glycylglycine, 40 mM HEPES, 5 mM EDTA, 5 mM EGTA (pH 8.0), 10 units/mL aprotinin, and 0.1 mM PMSF and homogenized with five up and down strokes of a 25 gauge needle on ice. Total cell lysate was then subjected to saturation binding analysis using [^{3}H]RX821002 as described above. Samples were normalized for the number of milligrams of protein using Bio-Rad's protein assay kit.

For pertussis toxin experiments, stably transfected EcR-CHO clones were treated with 200 ng/mL pertussis toxin in serum free medium for 24−36 h. Following treatment, cells were washed with PBS and scraped into 15 mM HEPES, 5 mM EDTA, 5 mM EGTA (pH 8.0), 10 units/mL aprotinin, and 0.1 mM PMSF and passaged with five up and down strokes using a 25 gauge needle on ice. Lysates were centrifuged at 40000*g* for 15 min followed by resuspension and recentrifugation. Pellets were then assayed for [^{125}I]-*p*-iodoclonidine ([^{125}I]PIC) binding in 50 mM Tris, 10 mM $MgCl_2$, and 5 mM EGTA (pH 8.0) or [^{3}H]RX821002 binding in 25 mM glycylglycine, 40 mM HEPES, 100 mM NaCl, and 5 mM EDTA (pH 8.0). Reactions were terminated via vacuum filtration as outlined above. [^{125}I]PIC binding was quantified using a Beckman γ counter. Samples were normalized for the number of milligrams of protein using Bio-Rad's protein assay kit as outlined above.

Western Analysis of Receptor Expression. Receptor was solubilized into an ice-cold solution containing 100 μL of 4 mg/mL dodecyl β-D-maltoside, 0.8 mg/mL cholesteryl hemisuccinate, 20% glycerol, 25 mM glycylglycine, 20 mM HEPES, 100 mM NaCl, 5 mM EGTA (pH8.0), 0.1 mM PMSF, and 10 units/mL aprotinin (called DβM/CHS extraction buffer). Receptor was solubilized via five up and down strokes with a 25 gauge needle on ice. Cellular debris was cleared from solubilized proteins by centrifuging at 13 000 rpm in a microfuge at 4 °C for 30 min. An aliquot (40 μL)

of the supernatant was subjected to 10% SDS−PAGE and transferred to nitrocellulose in a buffer containing 10 mM CAPS (pH 11.0) and 10% methanol for 1.2 h at 1 A. Nitrocellulose was blocked in Tris-buffered saline with 1% Tween 20 (TBST) containing 5% nonfat dry milk for 1 h at room temperature. HA-tagged receptor was then detected by blotting with a 1:1000 dilution of HA.11 primary antibody (BABCo) in blocking buffer followed by anti-mouse HRP-conjugated secondary antibody and ECL detection (Amersham).

Analysis of Cell Surface Residence Time for α_{2A}ARs. Transiently transfected cells were incubated with 10 μM idazoxan overnight to facilitate upregulation of D79N- and CAMα_{2A}AR protein for detection. Following overnight treatment, cells were washed three times with PBS at 37 °C to wash out the idazoxan and twice on ice with PBS at 4 °C and biotinylated at 4 °C with 1 mg/mL sulfo-NHS-biotin (Pierce) in PBS. Previous studies (*16*) have shown that this protocol results in labeling of surface residues only. Biotinylating at a single time point (defined as time zero) permits us to examine a single population of receptors present at the cell surface at time zero, without confounding our data with receptors newly delivered to the surface during the course of subsequent incubations. After biotinylation at 4 °C, cells were transferred to serum free medium at 37 °C with or without receptor ligand (10 μM idazoxan or 100 μM epinephrine in the presence of 100 μM ascorbate) and placed in a 5% CO_2 incubator at 37 °C. At the indicated time points, duplicate wells of a six-well plate were placed on ice and scraped into 1 mL of DβM/CHS extraction buffer per dish and passaged five times through a 25 gauge needle on ice. Cellular debris was cleared from solubilized protein via centrifugation at 13 000 rpm in a microfuge at 4 °C for 30 min. This supernatant was then incubated with 50 μL of streptavidin agarose overnight at 4 °C on an inversion wheel. The streptavidin agarose was washed twice with 0.5 mg/mL dodecyl β-D-maltoside, 0.1 mg/mL cholesteryl hemisuccinate in 25 mM glyclyglycine, 20 mM HEPES, 100 mM NaCl, and 5 mM EDTA (pH 8.0) (called DβM/CHS wash buffer) and eluted into 150 μL of SDS sample buffer for 15 min at 90 °C. These samples were then subjected to SDS−PAGE and Western analysis, as described previously. For semiquantitation of Western analyses, films were digitized by scanning into Adobe Photoshop and analyzed with NIH image software. Since the α_{2A}AR structures that were evaluated (wild type, D79N, CAM, and Δ3i) were quantitatively retained on streptavidin agarose, we interpret these findings to mean that all four receptor structures were exclusively on the cell surface.

Assessment of Receptor Binding and Protein Stability in Detergent-Solubilized Preparations. Transiently transfected COS M6 cells expressing wild type, D79N-, CAM-, or Δ3iα_{2A}AR were rinsed with PBS 48 h post-transfection. Cells were then biotinylated at room temperature with 1 mg/mL sulfo-NHS-biotin in PBS. The biotinylating solution was then aspirated, and cells were scraped on ice into ice-cold 15 mM HEPES, 5 mM EDTA, and 5 mM EGTA (pH 7.6) (with the addition of 10 units/mL aprotinin, 0.1 mM PMSF, 1 mg/mL soybean trypsin inhibitor, and 1 mg/mL leupeptin) and passaged five times up and down through a 25 gauge needle on ice. Lysates were then centrifuged at 40000*g* for 15 min at 4 °C. Pellets were resuspended on ice into DβM/CHS extraction buffer (with the addition of 10 units/mL aprotinin, 0.1 mM PMSF, 1 mg/mL soybean trypsin inhibitor, and 1 mg/mL leupeptin). Receptor was solubilized by 10 up and down strokes in a Teflon/glass homogenizer on ice. Cellular debris was cleared from solubilized protein by centrifugation at 13 000 rpm for 30 min at 4 °C. This supernatant fraction was defined as the detergent-solubilized receptor. At the given time points, following incubation at 25 °C, aliquots were removed and incubated with 40 μL of streptavidin agarose and 7.5 nM [^{3}H]yohimbine in DβM/CHS wash buffer (500 μL total reaction volume) at 4 °C on an inversion wheel for 1−1.5 h. Beads were then washed twice with DβM/CHS wash buffer. The remaining beads were then directly added to scintillation cocktail (Aquasol, Packard) and counted on a Packard scintillation counter. This biotin−streptavidin-dependent binding assay yielded identical results compared to those realized previously using Sephacel G-50 chromatography to separate bound from free ligand (*17*). To assess receptor stability over time, enough detergent-solubilized protein was added to the binding reaction mixtures to achieve 0.25−0.5 pmol of bound receptor at time zero (immediately following solubilization and clearance from cellular debris). Functional binding degradation was followed as a function of time by keeping the detergent-solubilized receptors at 25 °C and assaying the same volume of solubilized preparation per binding reaction at different time points. The stability of receptor protein in these same samples was confirmed by Western analysis of the HA epitope in the α_{2A}AR proteins using the HA.11 antibody, as described previously.

RESULTS

Uncoupling Receptor−G Protein Interactions Has No Effect on the Steady State α_{2A}AR Density Regardless of the Coupling Efficiency of the Receptor Structure Being Studied. Evaluation of a radiolabeled agonist:antagonist binding ratio can be used as an indirect readout of G protein coupling efficiency of a given receptor structure. [^{125}I]PIC:[^{3}H]-RX821002 binding ratios were determined for wild type, D79N-, and CAMα_{2A}AR structures expressed in CHO cells (Table 1), revealing that the altered coupling efficiencies for D79N (impaired coupling) and CAM (enhanced coupling) are recapitulated when these receptors are expressed in the CHO background. Additionally, pertussis toxin treatment, which uncouples receptor−G protein interactions, had no effect on the steady state receptor density of wild type, D79N-, or CAMα_{2A}AR despite eliminating high-affinity agonist binding (Table 1), an indirect readout of G protein coupling efficiency (*18*). Therefore, receptor−G protein coupling apparently plays no role in regulating the duration of α_{2A}AR protein expression regardless of the coupling efficiency of the receptor structure being evaluated.

Faster Surface $t_{1/2}$ for Δ3i-, D79N-, and CAMα_{2A}AR. Transient expression in CHO cells followed by evaluation of the surface $t_{1/2}$ of the wild type and Δ3iα_{2A}AR structures produced results nearly identical to those obtained for these structures on the basolateral surface of polarized MDCK II cells (Figure 2 and refs *8* and *9*), thus establishing this transient expression system for evaluating the mechanisms regulating α_{2A}AR surface $t_{1/2}$, mechanisms that can likely be generalized to other cell types. Evaluation of mutant

Table 1: Pertussis Toxin Has No Effect on Steady State α_{2A}AR Density, Regardless of the G Protein Coupling Efficiency of the Receptor Structure Being Monitored[a]

clone no.	R−G coupling efficiency (pmol of [^{125}I]PIC bound/pmol of [^{3}H]RX821002 bound)	R−G coupling efficiency (pmol of [^{125}I]PIC bound/pmol of [^{3}H]RX821002 bound and pertussis toxin bound)	% [^{3}H]RX821002 binding remaining and pertussis toxin remaining
wild type 86	0.18 ± 0.04	0.018 ± 0.004	87 ± 6.5
wild type 90	0.27 ± 0.015	0.027 ± 0.002	90 ± 9
CAM 15	0.37 ± 0.04	0.06 ± 0.004	87 ± 7
CAM 21	0.39 ± 0.08	0.062 ± 0.008	92 ± 8
D79N 59	0.05 ± 0.007	0.033 ± 0.004	89 ± 12
D79N 61	0.05 ± 0.009	0.033 ± 0.005	105 ± 6

[a] As an estimate of coupling efficiency, picomoles of [^{125}I]PIC bound/picomoles of [^{3}H]RX821002 bound ratios were determined (in the absence of pertussis toxin treatment). The amount of [^{125}I]PIC is a measure of the guanine nucleotide-sensitive high-affinity state of the α_{2A}AR and an indirect measure of R−G coupling efficiency, whereas the antagonist [^{3}H]RX821002 identifies all α_{2A}AR. Thus, the picomoles of [^{125}I]PIC bound/picomoles of [^{3}H]RX821002 bound ratio is reflective of the efficiency of coupling of the particular α_{2A}AR structure to G proteins. Consistent with other functional findings in the literature, CAMα_{2A}AR clones exhibit a higher ratio [due to constitutive activity (*15*)] and D79Nα_{2A}AR clones exhibit a lower ratio [in parallel with decreased coupling efficiency (*10*, *11*, *13*, *14*)]. Recalculation of the picomoles of [^{125}I]PIC bound/picomoles of [^{3}H]RX821002 bound ratio after pertussis toxin treatment reveals that R−G coupling has been disrupted. Percent [^{3}H]RX821002 remaining after pertussis toxin treatment (a readout of receptor density) represents the remnant receptor density after culturing cells for 24−36 h in the presence of 200 ng/mL pertussis toxin. Receptor densities were as follows (clone no. followed by B_{max} ± SE, K_D ± SE): clone 59, 0.83 ± 0.03 pmol/mg of protein and 1.8 ± 0.18 nM; clone 61, 2.0 ± 0.08 pmol/mg of protein and 3.2 ± 0.3 nM; clone 86, 2.4 ± 0.09 pmol/mg of protein and 2.5 ± 0.2 nM; clone 90, 0.87 ± 0.02 pmol/mg of protein and 1.4 ± 0.11 nM; and both CAM clones, 0.8 ± 0.05 pmol/mg of protein and 2 ± 0.15 nM.

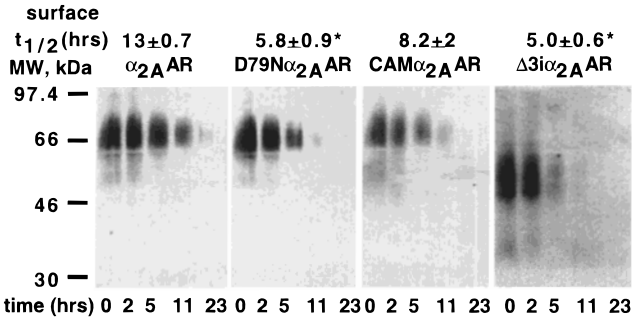

FIGURE 2: Evaluation of the surface $t_{1/2}$ of α_{2A}AR structures. Transiently transfected EcR-CHO cells were evaluated for surface turnover of expressed receptor using a cell surface biotinylation strategy (Experimental Procedures). Shown, for each receptor structure, is one representative Western analysis representative of three or four independent experiments. ANOVA reveals a p of <0.05, and an asterisk indicates a p of <0.05 using a Student−Newman−Keuls multiple-comparisons post test comparing wild type to D79N- and Δ3iα_{2A}AR surface $t_{1/2}$ values calculated using nonlinear regression curve fitting of semiquantitated Western analyses to the equation for a biological half-life [mean ± standard error (SE), n = 3−4]. The receptor densities in the absence of overnight treatment (defined as 100%) were as follows (mean ± SE in picomoles per milligram of protein): wild type, 1.4 ± 0.2; D79N, 0.42 ± 0.2; CAM, 0.3 ± 0.15; and Δ3i, 0.7 ± 0.2.

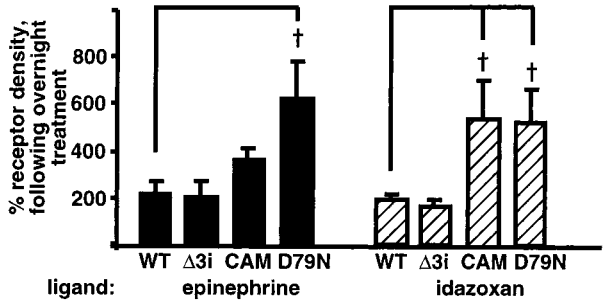

FIGURE 3: Dramatic ligand-dependent upregulation of steady state D79N- and CAMα_{2A}AR density in intact EcR-CHO cells. Transiently transfected cells were treated overnight with 100 μM epinephrine or 10 μM idazoxan as described in Experimental Procedures. The receptor density was determined using [^{3}H]-RX821002 saturation binding analysis and Western analysis (data not shown) 18−24 h after treatment. Shown is the mean percent change in receptor density ± SE (n = 3). ANOVA reveals a p of <0.05, and a dagger indicates a p of <0.05 using a Student−Newman−Keuls multiple-comparisons post test comparing wild type to D79N- or CAMα_{2A}AR density following the given overnight treatment. The receptor densities in the absence of overnight treatment (defined as 100%) were as follows (mean ± SE in picomoles per milligram of protein): wild type, 1.4 ± 0.2; D79N, 0.42 ± 0.2; CAM, 0.3 ± 0.15; and Δ3i, 0.7 ± 0.2.

α_{2A}ARs with known altered coupling efficiency revealed that the D79Nα_{2A}AR (reduced coupling) and CAMα_{2A}AR (enhanced coupling) both exhibited an accelerated surface turnover when compared to that of the wild type α_{2A}AR (Figure 2).

Ligand-Dependent Upregulation of D79N- and CAM- but Not Δ3i- or Wild Type α_{2A}AR. CAM receptors of multiple GPCRs, including CAM adrenergic receptors of the β_2AR (*19*, *20*), α_{1B}AR (*21*), and α_{2A}AR (*22*), have been shown to be able to undergo ligand-dependent upregulation of receptor density in a variety of cell types. As both CAM- and D79Nα_{2A}AR manifest altered G protein coupling efficiency (Table 1) and altered surface turnover (Figure 2), we sought to evaluate if ligand could modulate the steady state density of these receptors in cells. The D79Nα_{2A}AR density is upregulated dramatically with both agonist and antagonist when compared to that of the wild type (Figure 3). In contrast, the CAMα_{2A}AR density is significantly upregulated only by antagonist in an overnight treatment, when compared to that of the wild type receptor (Figure 3). The steady state receptor densities of wild type and Δ3iα_{2A}AR were not dramatically modulated by ligand occupancy (Figure 3).

Ligand-Dependent Surface Stabilization of D79N- and CAM- but Not Wild Type or Δ3iα$_{2A}$AR. To explain the cellular mechanisms resulting in the selective ligand-dependent upregulation of D79N- and CAMα_{2A}AR densities, we sought to evaluate the effect of ligand treatment on the surface stabilization of these four receptors. The presence of agonist or antagonist had no effect on the amount of surface-biotinylated wild type or Δ3iα_{2A}AR receptor remaining at 5 (Figure 4A) or 11 h (Figure 4B). However, both agonist and antagonist increased the amount of surface D79Nα_{2A}AR remaining at 5 and 11 h. In contrast, degrada-

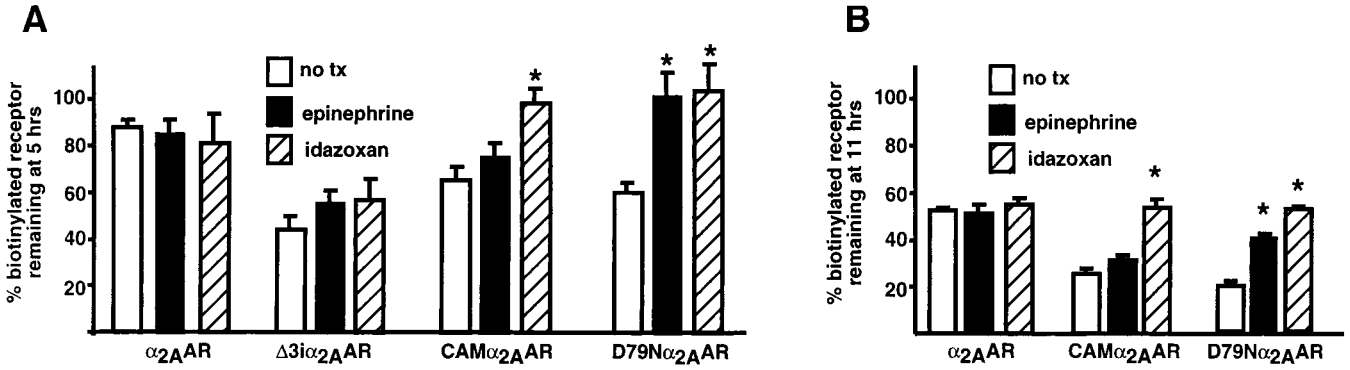

FIGURE 4: Selective ligand-dependent surface stabilization of D79N- and CAMα_{2A}AR turnover in intact EcR-CHO cells. Following surface biotinylation (Experimental Procedures), transiently transfected cells were treated with 100 μM epinephrine or 10 μM idazoxan and the effect of ligand on surface receptor turnover was evaluated. Western analysis of remaining biotinylated receptor at 5 (A) or 11 h (B) was semiquantitated with the use of NIH image software. Shown are the results of the percent biotinylated receptor remaining [mean ± SE (n = 3−4)] in the absence or presence of agonist or antagonist. ANOVA reveals a p of <0.05, and an asterisk indicates a p of <0.05 using a Student−Newman−Keuls multiple-comparisons post test comparing the percent biotinylated receptor remaining in the presence or absence of ligand for each receptor structure (D79N- or CAMα_{2A}AR).

tion of surface CAMα_{2A}AR was significantly inhibited only following antagonist occupancy of the receptor (Figure 4). Ligand-dependent slowing of the surface-to-degradation pathway for the D79N (by both agonist and antagonist)- and the CAMα_{2A}AR (by antagonist only) can explain the dramatic and selective ligand-dependent receptor density upregulation for these two receptor structures (Figure 3). This conclusion is supported by the lack of an effect of ligand on slowing surface turnover of the wild type α_{2A}AR or Δ3iα_{2A}-AR structures, for which there was also little effect of ligand on receptor density upregulation for these two receptor structures (Figure 3).

Structural Instability of D79N- and CAM- but Not Wild Type or D3iα_{2A}AR. Ligand-dependent slowing of surface receptor turnover and density upregulation for the D79N- and CAM- but not the wild type or Δ3iα_{2A}AR suggests a possible common mechanism regulating the surface $t_{1/2}$ of D79N- and CAMα_{2A}AR which is not being utilized for the wild type or Δ3iα_{2A}AR structures. Part of the explanation for the ligand-dependent upregulation of CAM receptors is thought to result from structural instability inherent to CAM receptor structures that can be stabilized by ligand occupancy (*19*, *20*, *23*). Structural instability has now been observed for two mutations within the β_2AR structure, each resulting in a CAM phenotype (*19*, *24*). As the D79Nα_{2A}AR also manifests ligand-dependent upregulation of receptor density, we sought to investigate the structural stability of the D79Nα_{2A}AR and compare it to those of wild type, Δ3i-, and CAMα_{2A}AR structures. An accepted method for evaluating the structural stability of GPCR structures appears to be measuring the loss of functional binding capacity in detergent solution over time compared to changes in receptor protein content over the same time period (*19*, *24*). Such an assay reveals inherent structural instability for the D79N- and CAMα_{2A}AR structures that is lacking in wild type or Δ3iα_{2A}-AR (Figure 5). The more rapid loss in functional binding capacity over time for the D79N- and CAMα_{2A}AR structures occurs in the context of no change in protein content comparing time zero to 2 h, indicating that the more rapid loss in binding capacity of the D79N- and CAMα_{2A}AR structures is due to structural instability and not proteolytic degradation.

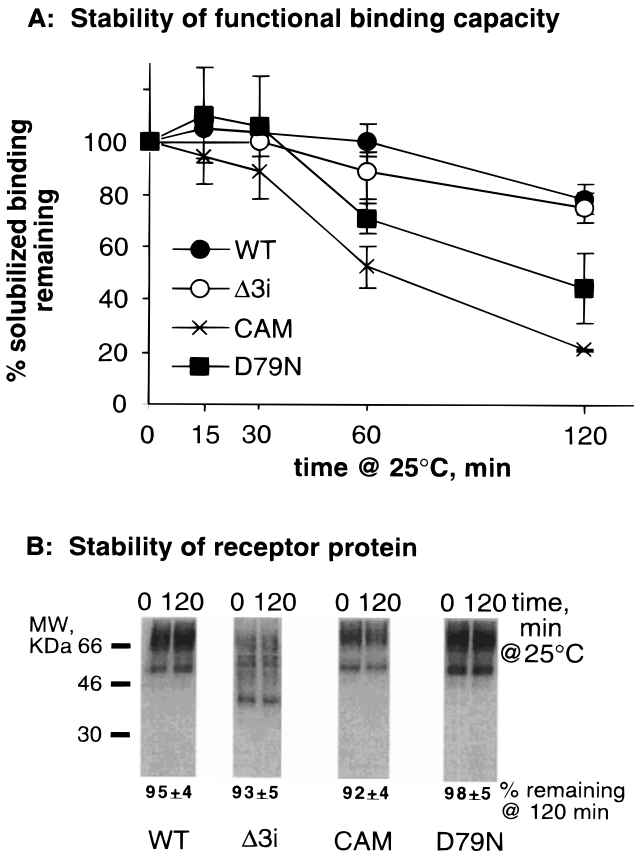

FIGURE 5: Structural instability of D79N- and CAMα_{2A}AR. (A) Conformational stability was measured by monitoring the loss of receptor binding following incubation at 25 °C in detergent-solubilized preparations. Receptors were extracted from COSM6 cells as described in Experimental Procedures, and binding was monitored using [^{3}H]yohimbine as the radioligand. Binding corresponded to 0.25−0.5 pmol of receptor at time zero. Shown is the mean percent ± SE from three independent experiments. (B) Western analysis reveals no receptor degradation comparing time zero to 120 min post-solubilization, revealing that the loss of binding is due to structural instability and not protein degradation. The data shown are means ± SE (n = 3). The wild type, D79N-, and CAMα_{2A}AR run at 66 kDa, and the Δ3iα_{2A}AR runs at 46 kDa. The lower-molecular mass bands likely represent incompletely processed receptor in COSM6 cells transiently expressing these receptor structures.

Table 2: Comparison of Receptor Properties of Wild Type and Mutant α_{2A}AR[a]

α_{2A}AR structure	G protein coupling[b]	surface $t_{1/2}$ (h)[c]	ligand-dependent surface stabilization[d]	ligand-dependent upregulation[e]	loss of binding capacity following detergent solubilization[f]
WT	WT	13 ± 0.7	little or none	little or none	stable
D79N	$\ll$WT	5.8 ± 0.9*	inc by ag/antag	inc by ag/antag	more rapid loss
CAM	$>$WT	8.2 ± 2	inc by antag only	inc by antag only	more rapid loss
Δ3i	$\sim$WT	5.0 ± 0.6*	little or none	little or none	stable

[a] A comparison of the functional properties of wild type and mutant α_{2A}AR structures reveals that structural instability, measured by the loss of functional binding capacity following detergent solubilization, also correlates with the extent of ligand-dependent surface stabilization, and the extent of ligand-dependent upregulation of receptor density, revealing that the altered surface $t_{1/2}$ for D79N- and CAMα_{2A}AR is due to structural instability. [b] G protein coupling represents the coupling capability of the receptor structure as determined in Table 1 or from previously published results [Δ3i (*8*)]. [c] Surface $t_{1/2}$ represents the cell surface half-life determined from Figure 2 (an asterisk denotes a statistically significant result as outlined in the Figure 2 legend). [d] Ligand-dependent surface stabilization (ag = agonist and antag = antagonist) was determined from Figure 4 (inc = increased). [e] Ligand-dependent upregulation from Figure 3. [f] Loss of functional binding capacity following detergent solubilization was determined in Figure 5.

DISCUSSION

A considerable literature has addressed the mechanisms regulating agonist-mediated removal of receptor from the cell surface, including evaluation of short-term agonist-mediated receptor internalization (sequestration) and agonist-mediated receptor degradation (downregulation). Proteins involved in regulating short-term agonist-mediated removal of receptor from the cell surface appear to include G protein-coupled receptor kinase (GRK), arrestin, and dynamin molecules (*2*, *5*, *25*, *26*); however, there also appear to be some short-term agonist-mediated internalization processes that are either GRK-, arrestin-, or dynamin-independent (*7*, *25*, *27*, *28*). As short-term agonist-mediated receptor sequestration may be linked to receptor downregulation (*6*, *29*, *30*), GRK, arrestin, and dynamin molecules have also been implicated in agonist-mediated receptor downregulation (*29*). However, some receptors appear to downregulate independent of short-term internalization (*31*); furthermore, arrestins may not be involved in receptor downregulation (*26*).

The current work began as an undertaking in an attempt to gain further understanding of the mechanisms regulating the long-term (hours) rather than short-term (minutes) surface retention and/or internalization of GPCRs, using the α_{2A}AR as a model for the superfamily of GPCRs. We report novel findings which show that mutational modification of a GPCR that alters inherent structural stability can result in cell surface turnover that is likely to be enhanced and can be modulated by receptor ligand. In this work, we have compared three different mutant α_{2A}AR structures (Table 2): (1) the Δ3iα_{2A}-AR, which manifests unaltered G protein coupling compared to that of wild type α_{2A}AR (*8*) but enhanced surface turnover that is not affected by ligand treatment resulting in little receptor density upregulation (Figures 2−4); (2) the D79Nα_{2A}-AR, which manifests impaired G protein coupling (Table 1) and enhanced surface receptor turnover that can be slowed with both agonist and antagonist as well as agonist- and antagonist-dependent receptor density upregulation (Figures 2−4); and (3) the CAMα_{2A}AR, which manifests enhanced G protein coupling (Table 1) and a trend of accelerated surface turnover that can be slowed only with antagonist as well as antagonist-only upregulation of receptor density (Figures 2−4). Presumably, the observed ligand-dependent stabilization of surface turnover and increase in receptor density observed for the D79N- and CAMα_{2A}AR are due to ligand stabilization of these inherently unstable receptor structures (Figure 5). Such a conclusion is supported by the lack of an effect of the ligand on surface turnover or steady state receptor density of the wild type or Δ3iα_{2A}AR, both of which have similar structural stability profiles (Figure 5).

The observation of structural instability for the D79Nα_{2A}-AR is intriguing. It is possible that the structural instability that results from this mutation explains the unexpected decrease in D79Nα_{2A}AR brain membrane density compared to wild type α_{2A}AR density in mice (*12*). Such a hypothesis is consistent with observed selective ligand-dependent upregulation of D79Nα_{2A}AR density in vivo.[2] Previous research has implicated a hydrogen bonding interaction between this conserved aspartate in transmembrane domain 2 (TM2) and a conserved asparagine in TM7 in regulating receptor activation (*32*, *33*). Mutation of this aspartate to asparagine could result in loss of this hydrogen bonding interaction, creating structural instability. The D79N mutation represents mutation of yet another residue postulated to be involved in receptor activation, such as the highly conserved aspartate in the DRY motif at the base of TM3 (*24*) or the residues at the base of TM6 in the β_2AR (*19*), which results in structural instability. For the CAMβ_2AR, structural instability is thought to contribute to constitutive activity (*19*); however, this is apparently not the case for the D79Nα_{2A}AR. Thus, although structural instability is observed for the D79N mutation, impaired rather than enhanced G protein coupling efficiency is observed (Table 1 and refs *10*−*14*). These findings suggest that mutations which alter G protein coupling (such as CAM or D79N) may result in structural instability regardless of whether coupling is enhanced or attenuated. Additionally, the dramatic effect of both agonist and antagonist on D79Nα_{2A}AR surface turnover and density versus the effect of only antagonist on these phenotypes for the CAMα_{2A}AR (Figures 3 and 4) implies a molecular difference underlying the observed structural instability of these two receptors. It is of interest that previous studies have demonstrated stabilization of the CAMβ_2AR by both agonist and antagonist (*19*, *24*). In contrast, CAM mutants of the α_{1B}AR (*21*) and α_{2A}AR (*22*) have previously been shown to undergo stabilization and/or upregulation in the presence of ligands acting as inverse agonists. It is possible that the CAMα_{2A}AR does not experience agonist-mediated stabilization because its conformation already mimics an agonist-bound or activated conformation, whereas the conformation(s) of the D79Nα_{2A}-AR can be stabilized by both agonist and antagonist (Figures

[2] M. H. Wilson and L. E. Limbird, unpublished observations.

3 and 4) because it mimics neither an active nor a classically inactive conformation. Without a three-dimensional receptor structure for these wild type and mutant receptors, we cannot resolve these hypothetical possibilities.

There are multiple possible mechanisms whereby structural instability imparted by mutation of a GPCR could lead to enhanced degradation of surface receptor. Molecules which serve as "chaperones" have been shown to be necessary for surface expression of GPCRs, including ninaA for rhodopsin (*34*), ODR-4 for odorant receptors (*35*), and RAMPs for the calcitonin receptor-like receptor (*36*). It has also been demonstrated that chaperonin molecules play a role in the maturation of membrane proteins such as the cystic fibrosis transmembrane regulator, and disruption of these interactions leads to enhanced proteolytic degradation of membrane proteins (*37*). Therefore, it is possible that mutations that alter the intrinsic structural stability of a GPCR could disrupt interactions with not-yet-determined molecules which serve as chaperones to stabilize the α_{2A}AR on the cell surface.

Additionally, ubiquitination has been shown to regulate the surface expression of GPCR in *Saccharomyces cerevisiae* and for various other cell surface receptors, transporters, and channels in mammalian cells (*38*). Structurally unstable surface-localized GPCR may be ubiquitinated and targeted for proteolytic degradation from the cell surface, although sequences that are critical for known unbiquitination pathways do not exist in the C-terminus of the α_{2A}AR. Interestingly, a recent report has demonstrated that downregulation of the β_2AR can occur at the plasma membrane independent of internalization of receptor in some cell types, implying the existence of plasma membrane proteases that can degrade GPCRs (*39*). The structural instability of a GPCR may enhance interaction with such plasma membrane proteases, resulting in receptor downregulation that may be modified by ligands which favor one protease-sensitive conformation versus another.

The observation that structural stability and instability can regulate the surface turnover of a GPCR represents an additional site of potential intervention in regulating the function of a GPCR. The fact that structural instability results in alteration of surface receptor turnover that can be modulated with ligand implies that there may exist cellular machinery which specifically recognizes and degrades structurally unstable receptors. As the surface residence time of a receptor population is important in GPCR function, blockade of such machinery or enhancement of the ability of this machinery to recognize and degrade GPCRs could be used as another method of regulating GPCR function. Additionally, small molecules which could serve to stabilize GPCR structure independent of traditional receptor specific ligands that regulate activity, whether peptide or small molecule in nature, could be used to regulate the surface expression of a given GPCR population and thereby modulate function.

ACKNOWLEDGMENT

We thank Robert J. Lefkowitz (Duke University, Durham, NC) for the gift of the CAMα_{2A}AR, Carol Ann Bonner for superior technical assistance, and all members of the Limbird lab for enthusiasm and helpful discussions.

REFERENCES

1. Limbird, L. E. (1988) *FASEB J. 2*, 2686−2695.
2. Lefkowitz, R. J. (1998) *J. Biol. Chem. 273*, 18677−18680.
3. von Zastrow, M., and Kobilka, B. K. (1992) *J. Biol. Chem. 267*, 3530−3538.
4. Daunt, D. A., Hurt, C., Hein, L., Kallio, J., Feng, F., and Kobilka, B. K. (1997) *Mol. Pharmacol. 51*, 711−720.
5. DeGraff, J., Gagnon, A., Benovic, J., and Orsini, M. (1999) *J. Biol. Chem. 274*, 11253−11259.
6. Eason, M. G., and Liggett, S. B. (1992) *J. Biol. Chem. 267*, 25473−25479.
7. Schramm, N. L., and Limbird, L. E. (1999) *J. Biol. Chem. 274*, 24935−24940.
8. Keefer, J. R., Kennedy, M. E., and Limbird, L. E. (1994) *J. Biol. Chem. 269*, 16425−16432.
9. Edwards, S. W., and Limbird, L. E. (1999) *J. Biol. Chem. 274*, 16331−16336.
10. Ceresa, B. P., and Limbird, L. E. (1994) *J. Biol. Chem. 269*, 29557−29564.
11. Surprenant, A., Horstman, D. A., Akbarali, H., and Limbird, L. E. (1992) *Science 257*, 977−980.
12. MacMillan, L. B., Hein, L., Smith, M. S., Piascik, M. T., and Limbird, L. E. (1996) *Science 273*, 801−803.
13. Lakhlani, P. P., Lovinger, D. M., and Limbird, L. E. (1996) *Mol. Pharmacol. 50*, 96−103.
14. Lakhlani, P. P., MacMillan, L. B., Guo, T. Z., McCool, B. A., Lovinger, D. M., Maze, M., and Limbird, L. E. (1997) *Proc. Natl. Acad. Sci. U.S.A. 94*, 9950−9955.
15. Ren, Q., Kurose, H., Lefkowitz, R. J., and Cotecchia, S. (1993) *J. Biol. Chem. 268*, 16483−16487.
16. Wozniak, M., and Limbird, L. E. (1996) *J. Biol. Chem. 271*, 5017−5024.
17. Nunnari, J. M., Repaske, M. G., Brandon, S., Cragoe, E. J., Jr., and Limbird, L. E. (1987) *J. Biol. Chem. 262*, 12387−12392.
18. Gerhardt, M. A., Wade, S. M., and Neubig, R. R. (1990) *Mol. Pharmacol. 38*, 214−221.
19. Gether, U., Ballesteros, J. A., Seifert, R., Sanders-Bush, E., Weinstein, H., and Kobilka, B. K. (1997) *J. Biol. Chem. 272*, 2587−2590.
20. Samama, P., Bond, R. A., Rockman, H. A., Milano, C. A., and Lefkowitz, R. J. (1997) *Proc. Natl. Acad. Sci. U.S.A. 94*, 137−141.
21. Lee, T., Cotecchia, S., and Milligan, G. (1997) *Biochem. J. 325*, 733−739.
22. Betuing, S., Valet, P., Lapalu, S., Peyroulan, D., Hickson, G., Daviaud, D., Lafontan, M., and Saulnier-Blache, J. S. (1997) *Biochem. Biophys. Res. Commun. 235*, 765−773.
23. Milligan, G., and Bond, R. A. (1997) *Trends Pharmacol. Sci. 18*, 468−474.
24. Rasmussen, S. G., Jensen, A. D., Liapakis, G., Ghanouni, P., Javitch, J. A., and Gether, U. (1999) *Mol. Pharmacol. 56*, 175−184.
25. Zhang, J., Ferguson, S. S. G., Barak, L. S., Menard, L., and Caron, M. G. (1996) *J. Biol. Chem. 271*, 18302−18305.
26. Zhang, J., Barak, L. S., Anborgh, P. H., Laporte, S. A., Caron, M. G., and Ferguson, S. S. (1999) *J. Biol. Chem. 274*, 10999−11006.
27. Vickery, R. G., and von Zastrow, M. (1999) *J. Cell Biol. 144*, 31−43.
28. Vogler, O., Bogatkewitsch, G. S., Wriske, C., Krummenerl, P., Jakobs, K. H., and van Koppen, C. J. (1998) *J. Biol. Chem. 273*, 12155−12160.
29. Gagnon, A. W., Kallal, L., and Benovic, J. L. (1998) *J. Biol. Chem. 273*, 6976−6981.
30. Nakamura, K., Lazari, M. F., Li, S., Korgaonkar, C., and Ascoli, M. (1999) *Mol. Endocrinol. 13*, 1295−1304.
31. Barak, L. S., Tiberi, M., Freedman, N. J., Kwatra, M. M., Lefkowitz, R. J., and Caron, M. G. (1994) *J. Biol. Chem. 269*, 2790−2795.
32. Zhou, W., Flanagan, C., Ballesteros, J. A., Konvicka, K., Davidson, J. S., Weinstein, H., Millar, R. P., and Sealfon, S. C. (1994) *Mol. Pharmacol. 45*, 165−170.
33. Sealfon, S. C., Chi, L., Ebersole, B. J., Rodic, V., Zhang, D., Ballesteros, J. A., and Weinstein, H. (1995) *J. Biol. Chem. 270*, 16683−16688.

34. Baker, E. K., Colley, N. J., and Zuker, C. S. (1994) *EMBO J. 13*, 4886−4895.
35. Dwyer, N. D., Troemel, E. R., Sengupta, P., and Bargmann, C. I. (1998) *Cell 93*, 455−466.
36. McLatchie, L. M., Fraser, N. J., Main, M. J., Wise, A., Brown, J., Thompson, N., Solari, R., Lee, M. G., and Foord, S. M. (1998) *Nature 393*, 333−339.
37. Loo, M. A., Jensen, T. J., Cui, L., Hou, Y., Chang, X. B., and Riordan, J. R. (1998) *EMBO J. 17*, 6879−6887.
38. Hicke, L. (1999) *Trends Cell Biol. 9*, 107−112.
39. Jockers, R., Angers, S., Da Silva, A., Benaroch, P., Strosberg, A. D., Bouvier, M., and Marullo, S. (1999) *J. Biol. Chem. 274*, 28900−28908.
40. Probst, W. C., Snyder, L. A., Schuster, D. I., Brosius, J., and Sealfon, S. C. (1992) *DNA Cell Biol. 11*, 1−20.

BI9920275